Three-Dimensional Modeling of a Chinese Circulating Fluidized Bed Incinerator Firing Municipal Solid Waste

Nikku Markku, Zhan Mingxiu, Myöhänen Kari, Ritvanen Jouni, Li Xiaodong

DOI: 10.5276/JSWTM/2021.393

Three-dimensional modeling of a Chinese circulating fluidized bed incinerator firing municipal solid waste

Markku Nikku*[a], Mingxiu Zhan[b], Kari Myöhänen[a], Jouni Ritvanen[a], Xiaodong Li[c]

a) LUT School of Energy Systems, Lappeenranta University of Technology, P.O. Box 20, FI-53851 Lappeenranta, Finland

b) College of Metrology and Measurement Engineering, China Jiliang University, Hangzhou, 310018, P.R. China

c) Institute of Thermal Power Engineering, State Key Laboratory of Energy Clean Utilization, Zhejiang University, Zheda Road 38, Hangzhou, 310027, P.R. China

*Corresponding author: Tel.: +358 40 501 5201, E-mail address: mnikku@lut.fi (M. Nikku).

Keywords: circulating fluidized bed, municipal solid waste, modeling, incineration, incinerator.

Abstract

Currently waste incineration is a widely used method of waste management in China. Effective incineration requires understanding and tools to analyze the incineration process leading to good incinerator performance and efficiency as well as lower emissions. In this work, a Chinese circulating fluidized bed (CFB) incinerator firing municipal solid waste (MSW) and coal is modeled with a three-dimensional CFB furnace model to evaluate the incineration process. First, the modeling results are verified with measurement data from the incinerator. Then, the furnace model is applied in the simulation of a case with more dry MSW without coal. The objective of the research is to provide insight and increase understanding of the MSW incineration process. The simulation case of MSW with the lower moisture content highlights the possible reductions of fossil carbon emissions associated with

the utilization of coal. To achieve this, a moderate reduction in the moisture content of MSW is required. A comparison between the MSW and coal versus only the MSW shows minor differences in the performance of the incinerator. Utilization of modeling in incinerator studies can aid in development of more efficient CFB incinerators, improving the waste management and reducing the utilization of fossil coal.

1 Introduction

The amount of waste produced by the society has been increasing in China along with the economic growth. At the same time, methods and policy for handling the amount of accumulating waste have to be developed, as only landfilling the waste is no longer considered as a viable option. (Nie 2008, Song et al 2016) The European Union has addressed this issue with a waste hierarchy, where the preferred option is the prevention of waste, followed by reuse, recycling, recovery and disposal as the last resort (European commission 2008). As waste generation cannot currently be avoided, and reuse and recycling of all materials is not always feasible, this leaves the recovery in form of energy as a viable option to reduce the amount of landfilled waste. The incinerators reduce the amount of solid waste by up to 80 %-volume or 70 %-mass (Li et al 2010), as the moisture, volatiles and fixed carbon are removed from the solid waste, leaving only the ash to be landfilled or postprocessed further. Due to this, there has been a significant increase in China in the number of incinerating plants for municipal solid waste (MSW) (Li et al 2016) as well as in the share of waste incinerated with a respective decline in the share of waste landfilled (Li et al 2015).

MSW consists of different waste fractions (such as paper, plastic, textile and wood for example) generated at various sources, such as households, offices and industry. The composition and properties of MSW have been shown to vary depending on the source

(Nasrullah 2015), seasons (Horttanainen et al 2013, Xiao et al 2009) and different countries as well as regions within a country (Zhiqiang et al 2005, Zhou et al 2014). Additionally, MSW can have low material density and it can contain a significant share of non-combustible fractions (such as soil, glass, metals or even hazardous materials) and organic material, such as food waste, which lower its quality as a fuel and increase the demand for fuel pretreatment. In particular, the Chinese MSW contains high shares of food waste (Zhou et al 2014), leading to high moisture content and lower heating value than in Europe (Nie 2008, Zhou et al 2014). The significant heterogeneity, along with the other previously mentioned features lead to challenges in MSW incineration.

Fluidized beds have certain advantages over other types of MSW incinerators. Incineration with circulating fluidized beds (CFB) can provide high combustion efficiency for solids and volatile gases, residence times over 2 s in temperatures exceeding 850°C (required by the European Commission (2010) and China (Chen et al 2010)) as well as reduced SO_x and NO_x emissions. Appropriate flue gas treatment methods have to be applied to ensure that the set requirements for gaseous and particulate emissions are achieved (Li et al 2016). Most importantly, fluidized beds can tolerate changes in the fuel quality, which enables the combustion of heterogeneous materials, such as untreated biomass or MSW. In 2006, 50 fluidized bed incinerators were operated in 24 different plants in China (Li et al 2016). Due to the low heating value and high moisture content of Chinese MSW, several Chinese fluidized bed incinerators use coal as a support fuel (Dong et al 2002, Patumsawad et al 2002, Suksankraisorn et al 2004), which in turn enables the possibility to sell electricity to reduce the operational and investment costs (Nie 2008). An alternative to co-combustion with coal is to increase the heating value of MSW by drying it prior to incineration (Li et al 2014).

Application of mathematical modeling enables the estimation of the CFB incinerator performance and emissions, and optimization of the incinerator design. Modeling can also be

used to provide insight on the many aspects of the CFB incinerator process and it can be utilized when investigating problems. Modeling is especially helpful when dealing with challenging fuels such as MSW, where the legislation demands certain process conditions and emission levels. As the nature of the flow and mixing in large-scale CFB incinerators is inherently three-dimensional, the modeling has to consider all three spatial dimensions. For large CFB furnaces and incinerators, time-dependent computational fluid dynamics (CFD) simulations are often too time consuming for engineering applications, and a common solution is to perform steady-state simulation to represent time-averaged conditions of the incinerator. Previously, this kind of modeling studies on CFB furnaces have been published utilizing an in-house three-dimensional CFB model frame to study combustion, gasification, and sorbent reactions in commercial and pilot scale CFB units (Hyppänen et al. 1991, Myöhänen et al 2011, Lyytikäinen et al 2011, Nikku et al 2014, Nikku et al 2016). While many works are found in the literature dealing with different aspects of MSW incineration (waste production, chemical properties, emissions, enviromental impacts, etc.), novel technologies dealing with MSW (pyrolysis, gasification, digestion, etc.) or system level studies (integration, life cycle assestments, etc.), only one three-dimensional modeling study was found in the literature dealing with large scale CFB incineration process for MSW, the work by Xie et al (2017). While their method provides detailed results, the approach was computationally expensive, 30 seconds of simulation time required approximately 40 days of computations.

In this work, a Chinese CFB waste incinerator firing MSW and coal is modeled with an in-house three-dimensional CFB furnace model to evaluate the incineration process. In previous works, the model frame has been applied and validated with diffent kinds of coals and biomasses, but not previously with MSW. In this work, the modeling results are verified with available measurement data from the incinerator plant to demonstrate the applicability of the

model frame for MSW material. After demonstrating the modeling capability, the furnace model is applied in simulation of the same CFB incinerator when the MSW is more dry and does not require utilization of coal as a support fuel. The objective of the research is to provide insight on the flow and reactions of MSW inside the incinerator for increased understanding of the incineration process. The simulation case of MSW with the lower moisture content highlights possible reductions of fossil carbon emissions associated with the elimination of coal. To achieve this, a moderate reduction in the moisture content of MSW is required. A comparison between the MSW and coal versus only the MSW shows the profiles of concentrations and reactions inside the incinerator leading to slightly different emissions after the incinerator. Utilization of three-dimensional modeling in incinerator studies can aid to develop more efficient CFB incinerators for MSW, aiding both in waste management and reduction of utilization of fossil coal in the incineration process.

2 Numerical methods

Proper modeling of flow and mixing in a CFB furnace or incinerator requires the consideration of all three spatial dimensions. For large CFB units, transient CFD simulations consume too many computational resources and time to be practical in engineering applications such as design. Time and resources can be saved by assuming a steady-state operation of a CFB unit and performing steady-state simulation to represent time-averaged conditions inside the furnace. This approach is taken in the in-house, three-dimensional CFB furnace model (Myöhänen et al 2011) utilized in this work. Additionally, the model frame utilizes semi-empirical models in solution of reactions of fuel, sorbent and various gaseous species, fragmentation of solid material, convective and radiative heat transfer, and flow dynamics. This steady-state semi-empirical approach enables simulations of CFB furnaces faster than with traditional CFD, while loss of small scale details and temporal effects does

not hinder the applicability of the simulation results in engineering type of applications. Compared to the method of Xie et al (2017), the simulations presented in this work offer less details but they can be obtained in couple of hours, making the approach suitable for engineering type of design and analysis applications. Myöhänen et al (2011) have presented a long and comprehensive description of the models and approaches utilized in the three-dimensional CFB furnace model, hence only a brief summary is presented here and the most relevant model equations are presented in Appendix 1.

The particle size distribution of solid materials are divided into six size fractions, with solid materials being considered are the inert bed material, fuel and sorbent. The fuel consists of char, volatiles, moisture, and ash. The fuel reactions (such as drying, gasification, devolatilization and combustion of char) are handled by the respective reaction models. In the model frame, the furnace is discretized into uniform block mesh with typical mesh sizes in order of 100,000 cells for large CFB units. Typical simulation times are in the order of hours to reach a converged solution of the whole furnace process.

Except the fuel, semi-empirical approach is employed in solution of the flow field of solids. The vertical distribution of solids in the core of the furnace is determined by an empirical correlation. In the horizontal direction, the solids are divided uniformly into the core and a dense wall-layer is superimposed near the incinerator surfaces. Mass exchange between the core and wall layer is modeled to present the internal circulation characteristics of CFB. Potential flow approach is then applied in the solutions of the velocity field of all solid material, expect for the fuel. The gas pressure and velocity fields are solved with a continuity equation and a simplified momentum equation for the gaseous phase. The conservation of species is modeled separately utilizing a dispersive modeling for mixing.

The flow of fuel is based on the solution of a momentum equation for the fuel phase, in which fuel's inertia, gravity, and drag force from the gaseous and solid phases are considered. The momentum exchange is one-way coupled; the fuel phase has no effect on the flow of gas and bed material. More details on fuel flow solution can be found at Nikku et al (2016) and in Appendix 1.

3 Simulation cases

A Chinese CFB incinerator with a duty of 40 MW_{th} firing MSW with coal as a secondary fuel was simulated at 100% load level. The mass share of coal is 5 % of the total fuel feeding, which is approximately 26 % of the fuel power in as fired state. There are secondary air inlets on the sidewalls of the lower incinerator for staged combustion. The incinerator contains no internal heat surfaces and the walls are refractory covered with no evaporator tubes. The superficial flue gas velocity at the freeboard was approximately 4 m/s.

The incinerator geometry was discretized with a uniform hexahedral block mesh with a total of 66,000 computational cells, with the computational cell being 0.2 m by 0.2 m by 0.2 m in x, y and z directions, respectively. Figure 1 illustrates the mesh of the incinerator with the relevant inlets and outlets. The utilized cell sizes are similar to previous simulations with the same in-house CFB furnace model (Nikku et al 2014, Nikku et al 2016) and the model frame was found to be insensitive to mesh size (Nikku et al 2014). Both the MSW and coal are fed to the incinerator from the front wall with boundary conditions for fuel inlet velocity $[v_x,v_y,v_z]$ of [0,1,-1] m/s and fuel dispersion coefficients were 0.2 m/s^2 and 0.05 m/s^2 for horizontal and vertical directions, respectively (Nikku et al 2014). The chemical composition and other properties of the fuels utilized in the incinerator were provided by the MSW incineration plant and they are presented in Tables 1 and 2.

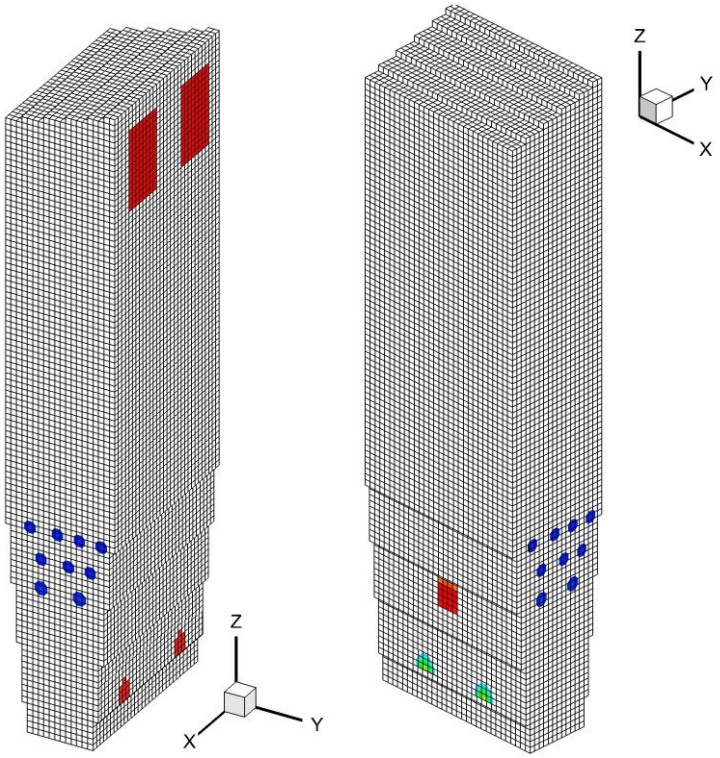

Figure 1. The simulated incinerator geometry with the computational mesh. On the left: the back wall with the separator inlets and solids return channels marked with red color. On the right: the front wall with the waste and coal feeding points marked with red and green, respectively. The secondary air inlets on the sidewall are marked with blue.

Table 1. Fuel properties. M, A, VM and FC are moisture, ash, volatile matter and fixed carbon, respectively, while C, H, O, N and S are content of carbon, hydrogen, oxygen, nitrogen and sulfur, respectively. The higher heating value (HHV) and ultimate analysis are represented on dry solids –basis while the proximate analysis is considered in as received –state.

	Proximate analysis [%-mass], ar				**Ultimate analysis [%-mass], ds**					**Other properties**	
	M	**A**	**VM**	**FC**	**C**	**H**	**O**	**N**	**S**	**HHV_{ds} [MJ/kg]**	**Material density [kg/m³]**
MSW	51.94	12.38	33.45	2.23	67.99	7.79	22.03	1.63	0.56	15.31	500
Coal	7.63	16.48	27.44	48.45	81.41	5.88	10.54	1.70	0.47	24.16	1300
Low moisture MSW	45.00	14.17	38.25	2.55	67.99	7.79	22.03	1.63	0.56	15.31	500

Table 2. Fractional particle size distribution of the fuels.

Fraction	**1**	**2**	**3**	**4**	**5**	**6**	**Unit**
Particle size	0.031	0.094	0.153	0.340	1.250	4.0	mm
MSW	0.01	0.02	0.1	4.87	15	80	%-mass
Coal	0.1	0.3	2.5	4	23.1	70	%-mass

Two cases were simulated: 1) A verified base case of the Chinese incinerator utilizing local MSW and coal, and 2) A hypothetical case identical to the base case expect for A) the moisture content of the MSW, which is decreased to 45 %, B) no coal is fed into the incinerator, as required temperature levels can be reached with the drier MSW. The base case was simulated first and the simulation model was verified with available measurement information. After the verification, the hypothetical case was simulated to investigate the incineration of only MSW without coal as a secondary fuel.

Keeping the simulation settings identical between the cases leads to a few small differences. The aim was to specify the hypothetical case so that it could be implemented in practice. The total amount of fuel utilized is slightly smaller in only MSW case compared to the base case. This results to approximately 1 MW lower thermal power of the incinerator, with reduced amount of char, and increased amounts of volatiles and ash. Additionally, the stoichiometric ratio for the air was kept the same as in the base case, which lead to small decrease in the amount of combustion air required. Overall, these differences are moderate, as the original mass share of coal was only 5 %.

4 Results and Analysis

For the verification case the overall incinerator mass and energy balances were satisfied and they correspond with the provided plant operating values. Measurement data of the simulated incinerator was used as verification material for the simulation results. The measurement and operational data was provided by the plant operator. The measurement results by Xie et al (2017) are qualitatively similar to the available measurement information used in this work, although the size of the incinerator is slightly larger and the share of coal and MSW is smaller in this work, with the most notable difference being the significantly higher moisture content of the MSW.

Figure 2 presents the simulated vertical temperature profiles corresponding with 5 of the available measurement points in different heights. Majority of the temperature measurements were located in the lower part of the incinerator. Overall, very good correspondence is achieved, on averages the difference is 2 % with a maximum difference of 8 %. Unfortunately, there is only one measurement point in the middle and the upper freeboard, though commonly the number of measurements points are very limited in commercial CFB units. In the upper freeboard the differences between measurement and modeled values are 5% and 1%, respectively. It can be seen that there are large local temperature gradients, especially near the MSW feeding region and secondary air inlets.

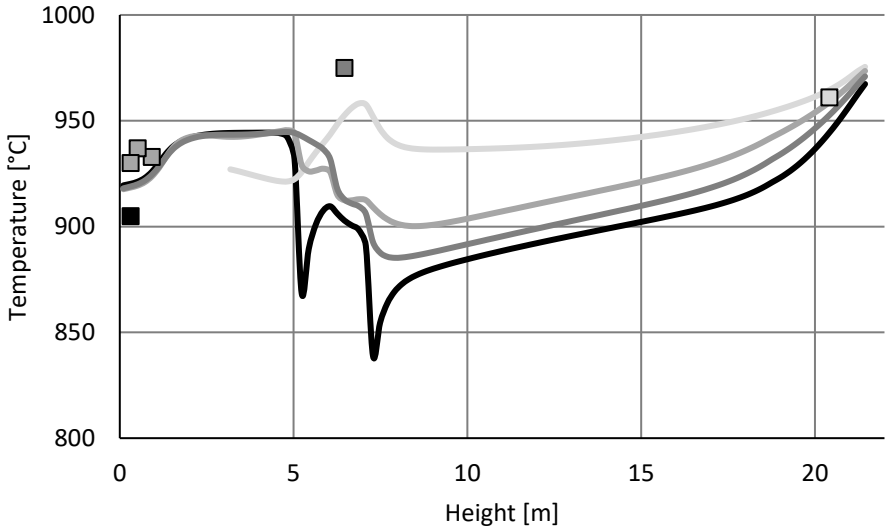

Figure 2. Modeled vertical temperature profiles, which relate to the different measurement points, presented in the same color.

Figure 3 presents the simulated, cross-sectionally averaged profiles of volumetric heat release (in kW/m^3). Heat released from the solid fuel is a sum of devolatilization and evaporation of moisture as well as gasification and combustion reactions of fuel char, while the heat release of gaseous species consists mainly of combustion reactions. Combined together these two form the total heat release profile. It can be seen that the solid fuel consumes energy due endothermic reactions of evaporation and devolatization of wet and high volatile MSW. The exothermic reactions of volatiles combustion provide the heat for the incinerator and lead to

mainly positive heat release, though from 2 to 5 meters the cross-sectional average of the total heat release is negative. This is due to limited gas combustion and feeding of the wet MSW to this height. Above 5 meters, the gas combustion increases due to the secondary air feeding, and together with lower concentrations of freshly fed MSW, the total heat release returns to positive. The effect of heat release in the upper parts of the incinerator is effectively larger due to increased volume compared to the tapered bottom part, ultimately leading to steady increase in the temperature in the upper part of the incinerator observed in Figure 5. The main differences between the two simulated cases are in the distribution of reactions of gaseous species and solids, with more even height wise distribution for gases and slightly lower total heat release in the case of using only MSW. The differences and three-dimensional distributions of the heat release are later presented in Figure 5.

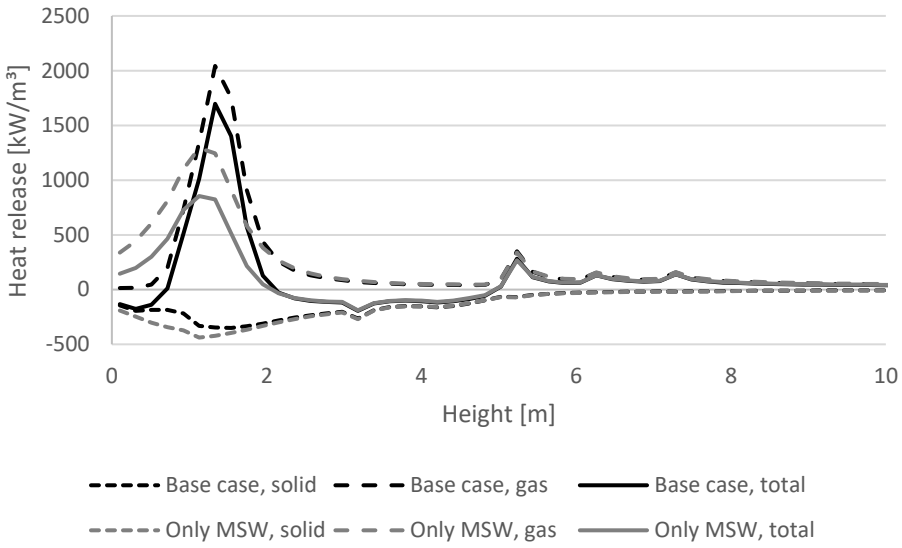

Figure 3. The averaged 1D profiles of heat release from the fuel in solid and gaseous states and the total released heat in kW/m³. The height is limited to the lower part of the incinerator where majority of reactions take place.

Figure 4 presents the three-dimensional distributions of major gaseous species concentrations and Figure 5 the three-dimensional temperature and combustion profiles of both the simulated cases. It can be seen for the base case, that near the MSW injection point the temperature distribution has a local cold spot and the local moisture content is very high. The wet injected MSW evaporates quickly near the inlet point and the energy required by the

244 evaporation causes the drop in the temperature, visible in the profiles presented in Figure 2
245 and Figure 3. The moisture content above MSW inlet point remain high, while the oxygen
246 and CO_2 concentrations are much lower. The char combustion occurs in the bottom of the
247 incinerator due to the coarse size and higher density of the coal particles does not allow them
248 to be transported higher in the incinerator. As most of the fuel is MSW and the majority of it
249 is volatiles, the combustion of volatile gases is mainly focused around the inlet point of
250 MSW. The mixing of the volatile gases and oxygen is limited, and there is an abundance of
251 volatile gases near the MSW inlet point, which lead to rapid consumption of oxygen as well
252 as oxygen deprived regions near and above the MSW inlet points. The volatile gases are only
253 able to combust when they come in contact with the oxygen closer to the sidewalls, which is
254 seen as a combustion front in the gas combustion profile. Especially the effect of secondary
255 air injection is illustrated well as the combustion of volatile gases reach their maximum. Due
256 to this incomplete mixing, a share of incombustible gases and char can exit the incinerator as
257 flue gas, as well as fly and bottom ash.

258

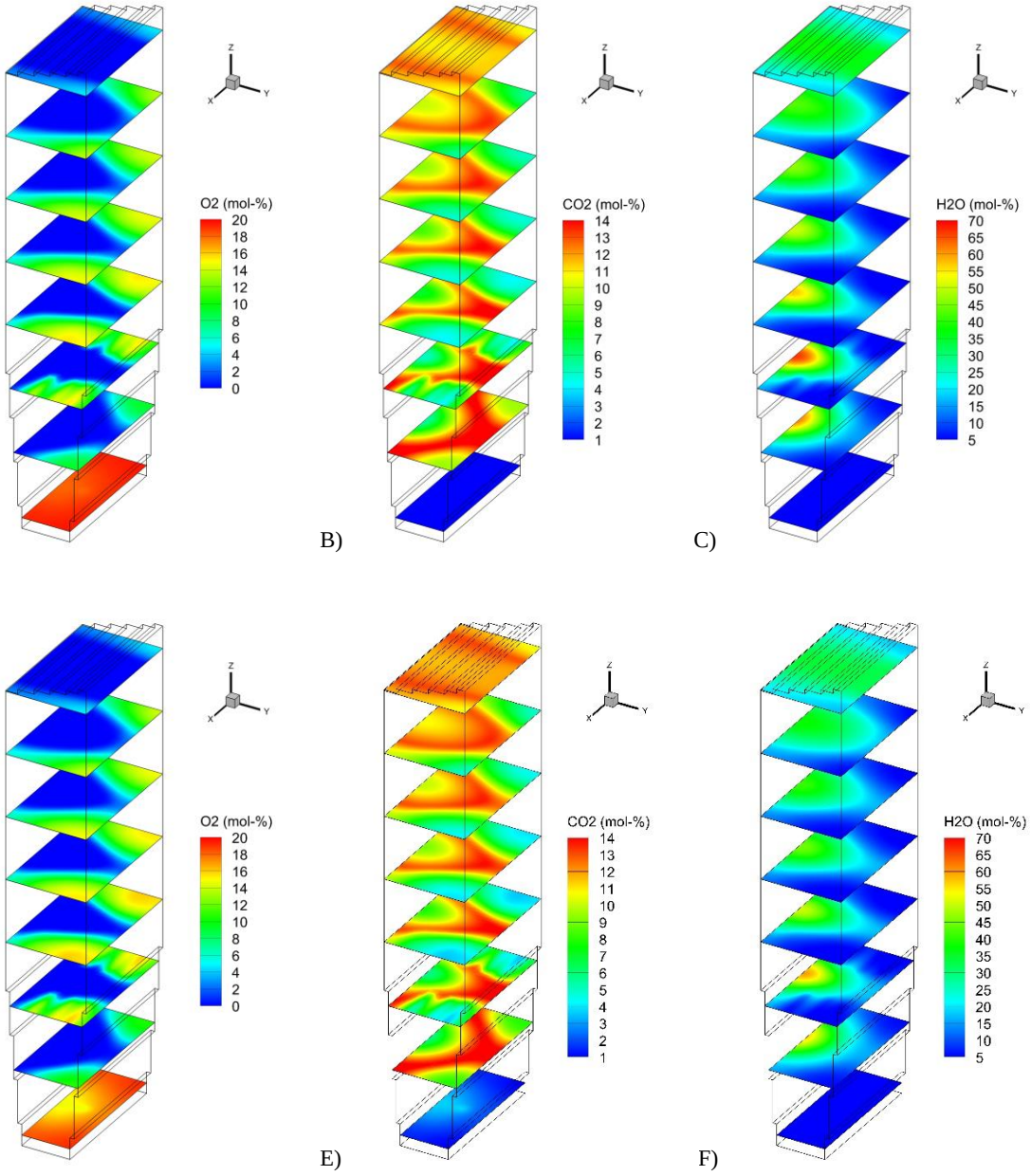

Figure 4. Concentration contours of oxygen, carbon dioxide and water vapor for the Chinese MSW and coal for the base case on the top (A-C) and dried MSW at the bottom (D-F).

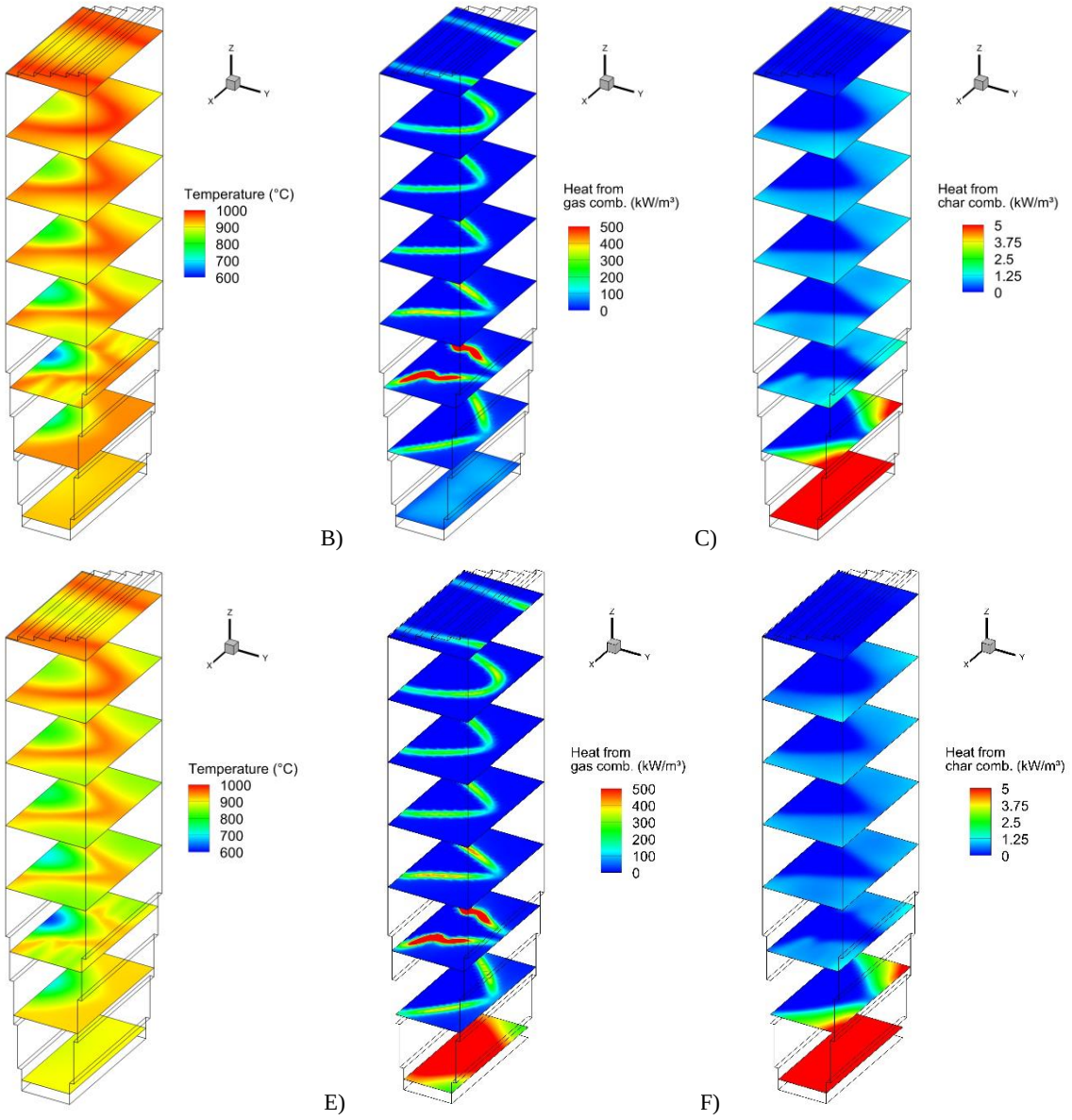

Figure 5. Contours of temperature, gas and char combustion for the Chinese MSW and coal for the base case on the top (A-C) and dried MSW at the bottom (D-F).

For the case with only the drier MSW, temperatures and the average temperature of the incinerator is lower, while still above 850°C required for waste incineration. Compared to the base case, the concentrations of the gaseous components change slightly with more oxygen remaining near the back wall corners, concentration of CO_2 are higher in the upper parts of the incinerator and moisture content is lower especially near the MSW inlet point. The combustion of volatiles occurs also in the lower part of the incinerator with similar combustion front visible as in the base case. Levels of volumetric char combustion are low

and very similar between the cases, only slightly lower for the only MSW case due to the reduced amount of char in the incinerator.

In both cases, the model predicts significant amount of unburned volatiles, due to limited mixing of combustion air and the volatiles. Table 3 presents the modeled results of the main gaseous emission species after the incinerator for both cases and the difference between the cases normalized by the mass flow rate of the flue gas, as only MSW case produces 2.5 % less flue gas. The amount of unburned volatiles increases 9.5 % in the case where only MSW is incinerated. This is also visible from Table 3, with a slight decrease in the end oxygen and a slight increase in all emission species, expect for NO which is halved, most likely due to lower incineration temperature. As the incinerator is likely designed to be operated with co-combustion of coal, it is expected to see slight drop in the performance in the case of only MSW. This is due to reduced amount of char and increased amount of volatiles compared to the base case. A redistribution of the MSW feeding or the secondary air nozzles could improve the mixing and volatile combustion leading more even oxygen distribution, combustion and temperature profiles as well as reduced amounts of unburned volatiles and lower emissions. At the same time, the reduced flue gas flow rate has an positive effect on the power plant performance, for example by lowering induced draft fan power consumption. Compared to the outlet gas composition reported by Xie et al (2017), the levels of oxygen and CO_2 are fairly similar with the emission components CO and SO2 of this work being some what smaller but in similar order of magnitude. The level of nitrous oxides are significantly lower, even though the nitrogen content of the fuels are higher. The differences can be explained by for example different reaction models and high temperature region near the fuel feeding in the case presented by Xie et al (2017), which increases the production of thermal NO_x.

299 **Table 3.** Modeled emissions before the flue gas treatment systems.

Emissions after cyclone scaled to 6% O_2, dry	**Base case**	**Only MSW**	**Normalized difference**
SO_2 (ppm,dry)	400	416	1.3 %
CO (ppm,dry)	1192	1351	9.5 %
NO (ppm,dry)	105	53	-102.6 %
N_2O (ppm, dry)	85	116	24.6 %
O_2 after the cyclone (%-mol, dry)	**5.23**	**5.33**	**-0.6 %**

300

301 # 5 Conclusions

302 A Chinese CFB incinerator for MSW co-firing coal was successfully modeled and the
303 modeling results were verified with available measurements from the incinerator plant. This
304 confirms that the three-dimensional CFB furnace model can be utilized in the modeling of
305 MSW incineration, which has not been previously done with the utilized model frame. This
306 enables the model frame to be utilized as a tool in further analysis and design of CFB MSW
307 incinerators.

308 The results indicate that by lowering the moisture content simulated Chinese MSW by 6 %-
309 mass, the incineration of MSW could be completed without utilization of fossil coal. This
310 would lead to significantly lower fossil carbon dioxide emissions and consumption of coal.
311 Taken that the MSW incineration is likely to increase in China as a method of waste
312 management, this translates to a significant reduction in the amount of fossile coal. In
313 practice, the lower moisture content could be achieved by implementing separation of food
314 wastes and by improving the waste collection. Additionally, thermal drying could be utilized
315 at the incineration site.

316 As shown, the CFB incinerators designed to fire MSW with coal as a support fuel can be
317 utilized in firing only MSW, with limited penalty in the incinerator performance. However, it
318 would be more beneficial to design the CFB incinerator for only MSW for maximum

combustion efficiency and to minimize the emissions. In this process, the utilized three-dimensional CFB furnace model would be a valuable tool to evaluate effects of different designs on the incinerator performance.

Obtaining representative average values for the properties and chemical composition of MSW is challenging due to large variations in, for example, the composition share of materials that form the bulk referred as MSW. In this study, the values used have been provided by the incineration plant and they represent the composition of the local MSW. A limited amount of measurement data is typically available for utilization in the model verification. However, a good agreement with the available temperature measurement indicates that there should be a reasonable agreement with other values, as the temperature profile is the results of distribution and reactions of gases and fuels inside the incinerator.

In the future, the three-dimensional CFB furnace model could be utilized in studying the placement of the fuel feeding and secondary air nozzles, to improve the mixing and volatile combustion for reducing the amount of unburned volatiles and decreasing the gaseous emissions.

Acknowledgments

This work was performed under the European Regional Development Fund project PAKUplus-HERGE (A70015).

Abbreviations

A	ash
C	carbon
CDW	construction and demolition waste
CFB	circulating fluidized bed
CWI	commercial and industrial waste
Cl	chlorine
FC	fixed carbon
H	hydrogen
M	moisture

MSW	municipal solid waste
N	nitrogen
O	oxygen
S	sulfur
VM	volatile matter

Symbols

A	area (m^2)
Ar	Archimedes number (-)
C	molar concentration (mol m^{-3})
C_D	drag coefficient
D	diffusion/dispersion coefficient (m^2 s^{-1})
E	activation energy (J mol^{-1})
H	height (m)
HHV	higher heating value (MJ kg^{-1})
K	momentum exchange coefficient (kg m^{-3} s^{-1})
Nu	Nusselt number (-)
P	flow potential (kg m^{-3} s^{-1})
Re	Reynolds number (-)
R	mass and species source term (kg m^{-3} s^{-1})
R_u	universal gas constant (8.3143 J mol^{-1} K^{-1})
S	source term in energy equation (W m^{-3})
T	temperature (°C)
V	volume (m^3)
X	molar fraction (-)
a	coefficient (–)
b	coefficient (–)
c	coefficient (–)
c_p	specific heat capasity at constant pressure (J kg^{-1} K^{-1})
d	diameter (m)
e	emissivity (-)
$\mathbf{g}$	gravitational acceleration (m s^{-2})
h	heat transfer coefficient (W m^{-2} K^{-1})
g_0	radial dispersion function (–)
k	rate coefficient (s^{-1})
p	pressure (Pa)
q	heat flow (W)
$\mathbf{v}$	velocity (m s^{-1})
w	mass fraction (–)
α	heat transfer coefficient (W m^{-2} K^{-1})
β	macroscopic drag coefficient (s^{-1})
ε	volume fraction (–)
θ	temperature difference to reference temperature (K)
μ	viscosity (kg s^{-1} m^{-1})
ρ	density (kg m^{-3})
σ	Stefan–Boltzman coefficient (W/m^2K^4)
ϕ	source term (kg m^{-3} s^{-1})
φ	switch function (–)

Subscripts

ar	as received
c	convection
ds	dry solids
E	Ergun
eff	effective
btm	bottom
dil	dilute
g	gas
H2O	water
fu	fuel
fri	friction
i, j	indexes
O2	oxygen
r	radiation
ref	reference
res	restitution
s	solid
susp	suspension
top	top
tot	total
trans	transition
w	wall
WY	Wen-Yu

References

Alakangas, E. 2000, Properties of fuels used in Finland (in Finnish), Technical Research Centre of Finland (VTT).

European commission. 2008. Directive 2008/98/EC (on waste and repealing certain Directives). Available online: http://eur-lex.europa.eu/legal-content/EN/TXT/PDF/?uri=CELEX:32008L0098&from=EN

European commission. 2010. Directive 2010/75/EU (on industrial emissions). Available online: http://eur-lex.europa.eu/LexUriServ/LexUriServ.do?uri=OJ:L:2010:334:0017:0119:en:PDF

Chen, X., Geng, Y., Fujita, T. 2010. An overview of municipal solid waste management in China, Waste Management 30, pp. 716-724.

Dong, C., Jin, B., Zhong, Z., Lan, J. 2002. Tests on co-firing of municipal solid waste and coal in a circulating fluidized bed, Energy Conversion and Management 43 (16), pp. 2189-2199.

Horttanainen, M., Teirasvuo, N., Kapustina, V., Hupponen, M., Luoranen, M. 2013. The composition, heating value and renewable share of the energy content of mixed municipal solid waste in Finland. Waste Management 33, pp. 2680-2686.

Huilin, L., Gidaspow, D. 2003. Hydrodynamics of binary fluidization in a riser: CFD simulation using two granular temperatures. Chemical Engineering Science 58, pp. 3777-3792.

Hyppänen, T., Lee, Y.Y., Rainio, A. 1991. A three-dimensional model for circulating fluidized bed boilers. In: Anthony. E.J.(Ed.), Proceedings of the 11th International Conference on Fluidized Bed Combustion.

Johnsson, F., Leckner, B. 1995. Vertical distribution of solids in a CFB-furnace. The 13th International Conference on Fluidized Bed Combustion. 7th-10th May 1995. Orlando, FL, USA.

Lebowitz, J. L. 1964. Exact solution of generalized Percus-Yevick equation for a mixture of hard spheres. Physical Review 133 (4A), pp. 895-899.

Li, G., Hu, Y. 2010. Comparisons of Municipal Solid Waste Incineration Residues Management in China and Europe, Proceedings of 2010 International Conference on Mechanic Automation and Control Engineering.

Li, S., Li, Y., Lu, Q., Zhu, J., Yao, Y., Bao, S. 2014. Integrated drying and incineration of wet sewage sludge in combined bubbling and circulating fluidized bed units, Waste Management 34 (12), pp. 2561-2566.

Li, Y., Zhao, X., Li, Y., Li, X. 2015. Waste incineration industry and development policies in China. Waste Management 46, pp. 234-241.

Li, X., Zhang, C., Li, Y., Zhi, Q. 2016. The Status of Municipal Solid Waste Incineration (MSWI) in China and its Clean Development. Energy Procedia 104, pp. 498-503.

Liu, J., Paode, R., Holsen, T. 1996. Modeling the Energy Content of Municipal Solid Waste Using Multiple Regression Analysis, Journal of the Air & Waste Management Association 46, pp. 650-656.

Liu, Z., Liu, Z., Li, X. 2006. Status and prospect of the application of municipal solid waste incineration in China. Applied Thermal Engineering 26, pp. 1193-1197.

Lyytikäinen, M., Kettunen, A., Myöhänen, K., Hyppänen, T., 2014. Utilization of a three dimensional model in designing and tuning of large scale boilers. In: Li. J., Wei. F., Bao. X., Wang, W.(Eds.), 11th International Conference on Fluidized Bed Technology.

Mack Rugg, F. 2012. Chapter 10.3 Physical and chemical characteristics, In: Chandrappa, R., Das, D.(Eds.), Solid Waste Management: Principles and Practice, Springer, ISBN: 978-3-642-28681-0.

Myöhänen, K., Hyppänen, T. 2011. A three-dimensional model frame for modelling combustion and gasification in circulating fluidized bed furnaces. Int. J. Chem. React. Eng. 9. A25, 55 p.

Myöhänen, K. 2011. Modelling of combustion and sorbent reactions in three-dimensional flow environment of a circulating fluidized bed furnace. Doctoral dissertation, Lappeenranta University of Technology.

Nasrullah, M. 2015. Material and energy balance of solid recovered fuel production. Doctoral dissertation, VTT Science 115. Available online: http://urn.fi/URN:ISBN:978-951-38-8368-3

Nie, Yongfeng. 2008. Development and prospects of municipal solid waste (MSW) incineration in China. Frontiers of Environmental Science and Engineering, China. 2(1), pp. 1-7.

Nikku, M., Myöhänen, K., Ritvanen, J., Hyppänen, T. 2014. Three-dimensional modeling of fuel flow with a holistic circulating fluidized bed furnace model. Chemical Engineering Science 117, pp. 352-363.

Nikku, M., Myöhänen, K., Ritvanen, J., Hyppänen, T. 2016. Three-dimensional modeling of biomass fuel flow in a circulating fluidized bed furnace with an experimentally derived momentum exchange model. Chemical Engineering Research and Design 115, pp. 77-90.

Patumsawad, S., Cliffe, K.R. 2002. Experimental study on fluidised bed combustion of high moisture municipal solid waste, Energy Conversion and Management 43 (17), pp. 2329-2340.

Schiller, L., Naumann, Z. 1935. Über die grundlegenden Berechnungen bei der Schwerkraftaufbereitung. Zeitschrift Des Vereines Deutscher Ingenieure 77, pp. 318–320.

Song, J., Yang, W., Li, Z., Higano, Y., Wang, X. 2016. Discovering the energy, economic and environmental potentials of urban wastes: An input–output model for a metropolis case, Energy Conversion and Management 114, pp. 168-179.

Suksankraisorn, K., Patumsawad, S., Vallikul, P., Fungtammasan, B., Accary, A. 2004. Co-combustion of municipal solid waste and Thai lignite in a fluidized bed, Energy Conversion and Management 45 (6), pp. 947-962.

Syamlal, M. Rogers, W., O'Brien, T. 1993. MFIX Documentation: Theory Guide. Morgantown Energy Technology Center.

Zhou, H., Meng, A., Long, Y., Li, Q., Zhang, Y. 2014. An overview of characteristics of municipal solid waste fuel in China: Physical, chemical composition and heating value. Renewable and Sustainable Energy Reviews 36, pp. 107-122.

Xiao, G., Ni, M., Chi, Y., Jin, B., Xiao, R., Zhong, Z., Huang, Y. 2009. Gasification characteristics of MSW and an ANN prediction model. Waste Management 29, pp. 240-244.

Xie, J., Zhong, W., Shao, Y., Liu, Q., Liu, L., Liu, G. 2017. Simulation of Combustion of Municipal Solid Waste and Coal in an Industrial-Scale Circulating Fluidized Bed Boiler, Energy Fuels 31, pp. 14248-14261.

Appendix 1. Relevant models of the three-dimensional CFB model frame, after Myöhänen (2011).

Continuity

1. Inert solids

Experimental vertical density profile fitted to equation by Johnsson et al (1995) which is applied for the whole cross section for each height *H*.

$$\varepsilon_{\mathrm{s}}(H)=\left(\varepsilon_{\mathrm{s,btm}}-\varepsilon_{\mathrm{s,top}}\exp\left(c_{\mathrm{dil}}H_{\mathrm{tot}}\right)\right)\exp\left(-c_{\mathrm{trans}}H\right)+\varepsilon_{\mathrm{s,top}}\exp\left(c_{\mathrm{dil}}\left(H_{\mathrm{tot}}-H\right)\right)$$

Continuity equation of inert solids: convection and source term.

$$\oint_A \varepsilon_{\mathrm{s}}\rho_{\mathrm{s}}\mathbf{v}_{\mathrm{s}}\cdot d\mathbf{A}=\int_V \phi_{\mathrm{s}}dV$$

2. Gas phase

Total gas equation continuity: convection and source terms.

$$\oint_A \varepsilon_{\mathrm{g}}\rho_{\mathrm{g}}\mathbf{v}_{\mathrm{g}}\cdot d\mathbf{A}=\int_V \phi_{\mathrm{g}}dV+\int_V R_{\mathrm{g}}dV$$

For gaseous species *i*: convection, diffusion and source terms.

$$\oint_A w_i\varepsilon_{\mathrm{g}}\rho_{\mathrm{g}}\mathbf{v}_{\mathrm{g}}\cdot d\mathbf{A}-\oint_A \varepsilon_{\mathrm{g}}\rho_{\mathrm{g}}D_{\mathrm{g}}\nabla w_i\cdot d\mathbf{A}=\int_V \phi_{\mathrm{g},i}dV-\int_V R_{\mathrm{g},i}dV$$

3. Fuel

For fuel size fraction *i*, continuity includes convection, diffusion, source terms and comminution between particle size fractions:

$$\oint_A \varepsilon_{\mathrm{fu},i}\rho_{\mathrm{fu},i}\mathbf{v}_{\mathrm{fu},i}\cdot d\mathbf{A}-\oint_A D_{\mathrm{fu},i}\nabla\left(\varepsilon_{\mathrm{fu},i}\rho_{\mathrm{fu},i}\right)\cdot d\mathbf{A}=\int_V \phi_{\mathrm{fu},i}dV-\int_V R_{\mathrm{fu},i}dV-\int_V \sum_{j,j\neq i}k_{\mathrm{fu},ij}\varepsilon_{\mathrm{fu},i}\rho_{\mathrm{fu},i}dV+\int_V \sum_{j,j\neq i}k_{\mathrm{fu},ji}\varepsilon_{\mathrm{fu},i}\rho_{\mathrm{fu},i}dV$$

Momentum

1. Inert solids

Potential flow approach is utilized.

$$\int_{\mathrm{V}} \varepsilon_{\mathrm{s}}\rho_{\mathrm{s}}\mathbf{v}_{\mathrm{s}}=\nabla P_{\mathrm{s}}$$

2. Gas

For the gas phase, a simplified momentum equation with macroscopic drag force is compensated by the pressure term.

$$\int_V \beta \varepsilon_s \rho_s \left(\mathbf{v}_g - \mathbf{v}_s\right) dV = -\int_V \varepsilon_s \nabla P dV$$

3. Fuel

The terms considered are inertia, gravity and buoyancy, drag from gas and solids (see Table A1 for used submodels) for fuel size fraction *i*:

$$\oint_A \varepsilon_{fu,i} \rho_{fu,i} \mathbf{v}_{fu,i} \mathbf{v}_{fu,i} \cdot d\mathbf{A} = \int_V \varepsilon_{fu,i} \left(\rho_{fu,i} - \rho_{susp}\right) \mathbf{g} dV + \int_V K_{g-fu,i} \left(\mathbf{v}_g - \mathbf{v}_{fu,i}\right) dV + \int_V K_{s-fu,i} \left(\mathbf{v}_s - \mathbf{v}_{fu,i}\right) dV$$

Reactions

1. Solid fuel

Volumetric reaction rate of fuel for all reactions (drying, devolatilization and char combustion), while each reaction is described by Arrhenius type of expression. In general, the effect of particle size compared to reference size, temperature and concentration of affecting species are considered.

$$R_{fu,i} = k_i \varepsilon_i \rho_i$$

1.1 Drying

$$k_i = a \left(\frac{d_p}{d_{ref}}\right)^b \exp\left(\frac{-E}{R_u T}\right)$$

1.2 Devolatilization

$$k_i = a \left(\frac{d_p}{d_{ref}}\right)^b \exp\left(\frac{-E}{R_u T}\right) \left(1 - w_{H2O}\right)^c$$

1.3 Char combustion

$$k_i = a \left(\frac{d_p}{d_{ref}}\right)^b \exp\left(\frac{-E}{R_u T}\right) C_{O2}^c$$

2. Reactions of gaseous species

Reactions of gaseous species is described by Arrhenius type of equation with the reaction rate depending on molar fractions X of participating species, ratio of pressure p to reference pressure p_{ref} and temperature T.

$$R_{\mathrm{g},i} = k_i \prod_l X_l^a \left(\frac{p}{p_{\mathrm{ref}}} \right)^b \exp\left(\frac{-E_i}{\mathrm{R_u} T} \right)$$

Table A1. The momentum exchange models.

Phenomenon	Model	Reference
Momentum exchange between gas and solids	$K_{\mathrm{g-s}} = \varphi K_{\mathrm{E}} + (1-\varphi) K_{\mathrm{WY}}$	
Dilute suspension	$K_{\mathrm{WY}} = \frac{3}{4} C_{\mathrm{D}} \frac{\varepsilon_{\mathrm{s}} \varepsilon_{\mathrm{g}} \rho_{\mathrm{g}} \lvert \mathbf{v}_{\mathrm{g}} - \mathbf{v}_{\mathrm{s}} \rvert}{d_{\mathrm{s}}} \varepsilon_{\mathrm{g}}^{-2.65} \quad \varepsilon_{\mathrm{g}} > 0.8$	Huilin et al (2003)
Dense suspension	$K_{\mathrm{E}} = 150 \frac{\varepsilon_{\mathrm{s}} (1-\varepsilon_{\mathrm{g}}) \mu_{\mathrm{g}}}{\varepsilon_{\mathrm{g}} d_{\mathrm{s}}^2} + 1.75 \frac{\rho_{\mathrm{g}} \varepsilon_{\mathrm{s}} \lvert \mathbf{v}_{\mathrm{g}} - \mathbf{v}_{\mathrm{s}} \rvert}{d_{\mathrm{s}}} \quad \varepsilon_{\mathrm{g}} \le 0.8$	
Switching function	$\varphi = \arctan[150 \cdot 1.75 (0.2 - \varepsilon_{\mathrm{s}})] \pi^{-1} + 0.5$	
Drag coefficient	$C_{\mathrm{D}} = \begin{cases} \frac{24}{\mathrm{Re}} (1 + 0.15\,\mathrm{Re}^{0.687}) & \mathrm{Re} \le 1000 \\ 0.44 & \mathrm{Re} > 1000 \end{cases}$	Schiller et al (1935)
Momentum exchange between solids phases	$K_{\mathrm{s},i-\mathrm{s},j} = \frac{3(1+c_{\mathrm{res}})(\pi/2 + c_{\mathrm{fri}} \pi^2/8) \varepsilon_{\mathrm{s},i} \varepsilon_{\mathrm{s},j} \rho_{\mathrm{s},i} \rho_{\mathrm{s},j} (d_{\mathrm{s},i} + d_{\mathrm{s},j})^2 g_0 \lvert \mathbf{v}_{\mathrm{s},i} - \mathbf{v}_{\mathrm{s},j} \rvert}{2\pi (\rho_{\mathrm{s},i} d_{\mathrm{s},i}^3 + \rho_{\mathrm{s},j} d_{\mathrm{s},j}^3)}$	Syamlal et al. (1993)
Radial distribution	$g_0 = \frac{1}{\varepsilon_{\mathrm{g}}} + \frac{3 d_{\mathrm{s},i} d_{\mathrm{s},j}}{\varepsilon_{\mathrm{g}}^2 (d_{\mathrm{s},i} - d_{\mathrm{s},j})} \left(\frac{\varepsilon_{\mathrm{s},i}}{d_{\mathrm{s},i}} + \frac{\varepsilon_{\mathrm{s},j}}{d_{\mathrm{s},j}} \right)$	Lebowitz (1964)

Energy equation

Energy equation is shared for both phases and includes terms for diffusion, sources and heat transfer to surfaces.

$$\oint_A \varepsilon_{\mathrm{g}} \rho_{\mathrm{g}} c_{\mathrm{pg}} T_g \mathbf{v}_{\mathrm{g}} \cdot d\mathbf{A} + \oint_A \varepsilon_{\mathrm{s}} \rho_{\mathrm{s}} c_{\mathrm{ps}} T_{\mathrm{s}} \mathbf{v}_{\mathrm{s}} \cdot d\mathbf{A} - \oint_A \varepsilon_{\mathrm{g}} \rho_{\mathrm{g}} D_g c_{\mathrm{pg}} \nabla T_{\mathrm{g}} \cdot d\mathbf{A} - \oint_A \varepsilon_{\mathrm{s}} \rho_{\mathrm{s}} D_s c_{\mathrm{ps}} \nabla T_{\mathrm{s}} \cdot d\mathbf{A} = \int_V S dV - \oint_A \alpha (T - T_w) \cdot d\mathbf{A}$$

1. Heat transfer

The total heat flux from the furnace to the wall is a sum of radiative and convective heat transfer. Radiation is considered to originate from the computational cells in the core region, where as the convection considers only the wall layer cells near the furnace wall. θ represents the difference of the temperature in cell *i* to the reference temperature.

$$q_{tot} = \oint_A \left[\mathbf{h}_{\mathrm{r}}\left(\theta_i - \theta_{\mathrm{w}}\right) + \mathbf{h}_{\mathrm{c}}\left(\theta_{\mathrm{wl}} - \theta_{\mathrm{w}}\right)\right] \cdot d\mathbf{A}$$

Heat transfer coefficient of radiative heat transfer between the wall and cell *i* is solve with effective emissivity e_{eff} and Stefan-Boltzmann constant:

$$h_r = \frac{e_{\mathrm{eff}}\,\sigma\left(T_i^4 - T_{\mathrm{w}}^4\right)}{T_i - T_{\mathrm{w}}}$$

The convective heat transfer coefficient is determined from empirical correlation with the suspension densities of the wall layer cell:

$$\mathrm{Nu}_c = \mathrm{Ar}^{0.25}\sqrt{\frac{\varepsilon\rho_{\mathrm{g}} + (1-\varepsilon)\rho_{\mathrm{s}}}{\rho_{\mathrm{s}}}}$$